REGULAR ARTICLE

# Soil $CO_2$ efflux and production rates as influenced by evapotranspiration in a dry grassland

**János Balogh · Szilvia Fóti · Krisztina Pintér ·
Susanne Burri · Werner Eugster · Marianna Papp ·
Zoltán Nagy**

**Abstract**

*Aims* Our aim was to study the effect of potential biotic drivers, including evapotranspiration (ET) and gross primary production (GPP), on the soil $CO_2$ production and efflux on the diel time scale.

*Methods* Eddy covariance, soil respiration and soil $CO_2$ gradient systems were used to measure the $CO_2$ and $H_2O$ fluxes in a dry, sandy grassland in Hungary. The contribution of $CO_2$ production from three soil layers to plot-scale soil respiration was quantified. $CO_2$ production and efflux residuals after subtracting the effects of the main abiotic and biotic drivers were analysed.

*Results* Soil $CO_2$ production showed a strong negative correlation with ET rates with a time lag of 0.5 h in the two upper layers, whereas less strong, but still significant time-lagged and positive correlations were found between GPP and soil $CO_2$ production. Our results suggest a rapid negative response of soil $CO_2$ production rates to transpiration changes, and a delayed positive response to GPP.

*Conclusions* We found evidence for a combined effect of soil temperature and transpiration that influenced the diel changes in soil $CO_2$ production. A possible explanation for this pattern could be that a significant part of $CO_2$ produced in the soil may be transported across soil layers via the xylem.

**Keywords** Diel timescale · Evapotranspiration · Gross primary production · Soil $CO_2$ production · Time series analysis

J. Balogh (✉) · K. Pintér · Z. Nagy
Institute of Botany and Ecophysiology, Szent István University, Páter u. 1, 2100 Gödöllő, Hungary
e-mail: Balogh.Janos@mkk.szie.hu

J. Balogh · S. Burri · W. Eugster
Grassland Sciences Group, Institute of Agricultural Sciences, ETH Zurich, Universitätsstrasse 2, 8092 Zürich, Switzerland

S. Fóti · M. Papp · Z. Nagy
MTA-SZIE Plant Ecology Research Group, Szent István University, Páter u. 1, 2100 Gödöllő, Hungary

## Introduction

Although evapotranspiration is a key process in ecosystem functioning and has global significance, it was only recently found that it may play a direct and significant role in carbon cycling between the plants and the soil by decreasing root respiration rates (Bekku et al. 2011; Grossiord et al. 2012). Thus, evapotranspiration could have a direct influence on soil $CO_2$ efflux. Soil $CO_2$ efflux was typically related to air or soil temperature ($T_s$), sometimes to soil water content (SWC), and in more recent cases to substrate supply (Lloyd and Taylor 1994; Parkin and Kaspar 2003; Carbone et al. 2008; Kuzyakov and Gavrichkova 2010; Balogh et al. 2011). However, abiotic and biotic factors affecting soil $CO_2$ efflux are acting on different temporal scales and

are interacting with each other (Vargas et al. 2010; Savage et al. 2013). Although the need for a proper mechanistic approach to model the effects of the drivers of soil respiration is obvious (Blagodatsky and Smith 2012), the effect of drivers acting on the diel timescale are still poorly understood. New measurement devices and methods, such as soil $CO_2$ sensors and automated soil respiration systems, provided new insights into soil carbon fluxes (Carbone and Vargas 2008). These methodological advances allowed measurements of soil $CO_2$ fluxes with a frequency, which is adequate and necessary for the analysis of diel patterns (Martin et al. 2012; Savage et al. 2013).

Previous studies typically focused on the decomposition aspect of soil respiration ($F_s$) dealing with the effect of $T_s$ and SWC. The effect of $T_s$ on $F_s$ has been extensively studied and used as a basis for soil respiration models in spite of its possible artefacts (Subke and Bahn 2010). The often observed phenomenon of hysteresis in the diel temperature response of soil respiration was usually linked to the different depths of $CO_2$ production and that of $T_s$ measurements according to a number of studies (Pavelka et al. 2007; Ruehr et al. 2009; Savage et al. 2013; Eler et al. 2013). The hysteresis effect increases the uncertainty of the often applied temperature response of soil or ecosystem respiration, and thus also increases the uncertainties of models and data gap-filling procedures. $F_s$ response to SWC can modify the temperature response, especially in dry ecosystems (Carbone et al. 2008; Lellei-Kovács et al. 2011; Fóti et al. 2014). Recent studies proposed parabolic (Moyano et al. 2013) or log-normal relationships (Balogh et al. 2011) for describing the effect of SWC, developed principally at low and high water contents (Davidson et al. 2012).

Biotic drivers represent the supply-side control in soil respiration models. Biotic drivers that integrate over longer time periods, like biomass, relative growth rate and vegetation indices (Jia and Zhou 2009; Huang and Niu 2012) are useful in describing the phenological changes and physiological state of the vegetation. However, these drivers are not suitable to explain the diel variability of soil respiration. In fact, two additional processes could be relevant on the diel timescale, acting in opposite directions: (1) photosynthesis, and (2) transpiration. Firstly, a time-lagged positive effect of photosynthesis on the respiration of roots and root-associated microbes on the order of hours were found by Mencuccini and Hölttä (2010), who explain this with

the increase in easily accessible non-structural hydrocarbon sources for the roots and root-associated organisms. Secondly, it was found that the effect of transpiration could reduce root respiration (Aubrey and Teskey 2009; Bloemen et al. 2013a), and this effect is expected to be immediate (i.e. without hysteretic delay).

Removing the effect of the abiotic drivers from the soil efflux signal has helped to clarify the role of other driving variables (Martin et al. 2012). So far, this has been done by multi-temporal correlation approaches (Vargas et al. 2011), by applying better experimental arrangement and data analysis (Graf et al. 2008), and by the proper vertical partitioning of the soil $CO_2$ production (Davidson et al. 2006a). Since the supply-side control on $F_s$ modifies its response to abiotic drivers, this effect could be detected by using residuals of soil respiration models (Balogh et al. 2011).

To test this, a combined approach was used in this study. We used automated systems: (i) eddy covariance, (ii) soil respiration, and (iii) soil gradient systems to analyse the effect of the different drivers on the soil $CO_2$ production and efflux. By measuring $CO_2$ concentration gradients in three soil layers, source attribution to these layers was possible. A correlation analysis was used to find relationships with gross primary production (GPP) and evapotranspiration (ET), both representing biotic drivers that potentially could significantly influence total soil respiration. Our research goal was to investigate whether and to what extent evapotranspiration modifies observed soil $CO_2$ production and efflux rates in grasslands.

## Materials and methods

### Site characteristics

The vegetation at the Bugac site (46.69° N, 19.6° E, 114 m above sea level) is a semi-arid sandy grassland dominated by *Festuca pseudovina*, *Carex stenophylla* and *Cynodon dactylon*. Mean annual precipitation of the last ten years (2004–2013) was 575 mm, and the mean annual temperature reached 10.4 °C. The soil is a chernozem type sandy soil with high organic carbon content (Table 1).

The study site is located in the Kiskunság National Park and has been under extensive management (grazing) for the last 20 years. The site was grazed occasionally by cattle from the end of April until the

**Table 1** Soil characteristics: soil texture, total nitrogen (TN), total organic carbon (TOC), pH, root biomass, organic matter (OM), bulk density (BD) and total porosity (φ). Eight replicates of soil cores of 15 cm diameter were collected from four depths at the end of the vegetation season on 29th September 2011

| depth | Sand (%) | Silt (%) | Clay (%) | TN (%) | TOC (%) | pH (KCl) | Root (kg m$^{-3}$) | OM (%) | BD (g cm$^{-3}$) | φ (m$^3$ m$^{-3}$) |
|---|---|---|---|---|---|---|---|---|---|---|
| 0–10 | 81.18 | 10.79 | 8.03 | 0.19 | 5.76 | 7.22 | 15.15 | 9.89 | 0.998 | 0.605 |
| 10–30 | 81.11 | 9.62 | 9.27 | 0.11 | 1.32 | 7.39 | 9.27 | 2.21 | 1.55 | 0.408 |
| 30–50 | 83.24 | 7.51 | 9.24 | 0.03 | 0.64 | 7.92 | 3.86 | 1.04 | 1.59 | 0.395 |
| 50–80 | 81.42 | 10.25 | 8.32 | 0.01 | 0.71 | 8.15 | 1.51 | 1.16 | 1.66 | 0.37 |

end of November in each year. Grazing pressure was about 0.75 animal ha$^{-1}$ during the study period.

Gas exchange measuring systems

The three different gas exchange systems used in this study provided data with different levels of spatial integration; the size of the eddy covariance (EC) flux footprint area was larger by several orders of magnitude than the area covered by the soil respiration system (SRS) or the gradient system. The variables derived from EC flux measurements (Fig. 1, GPP, ET) were considered as biotic drivers of soil $CO_2$ production rates. Greatest care was taken during the establishment of the experiment to select a part of the EC footprint area with the same average soil characteristics and vegetation composition and cover found in the plots where the SRS and gradient systems were installed. Hence, the GPP and ET estimates obtained in this way can be considered representative also for the small-scale SRS and gradient system measurements.

Data from July 2011 to November 2012 were analysed in this study.

*Eddy covariance setup*

The EC system at the Bugac site has been measuring the $CO_2$ and $H_2O$ fluxes continuously since 2002. In dry
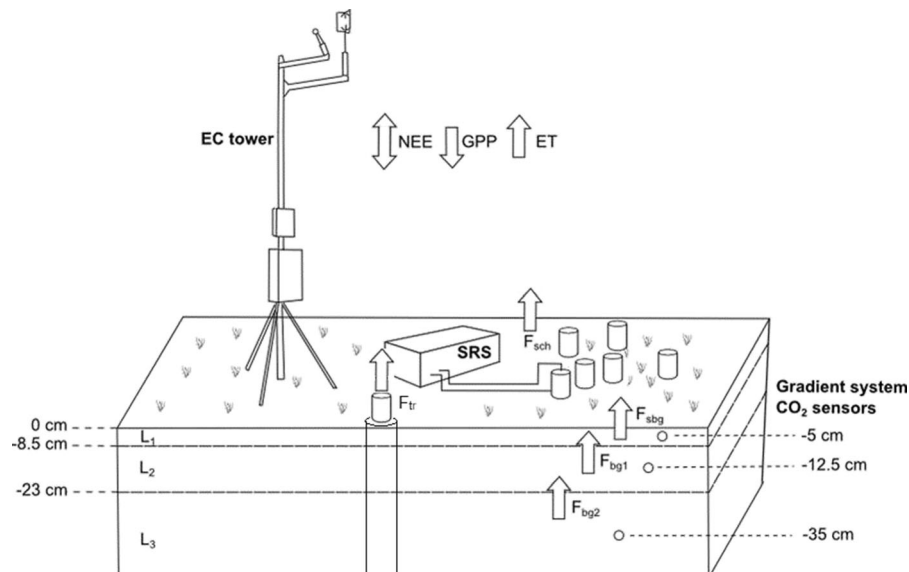


**Fig. 1** Experimental setup to measure the different gas fluxes within and over the soil. EC tower: eddy covariance system for measuring net ecosystem exchange of $CO_2$ (NEE), gross primary production (GPP), evapotranspiration (ET) and climatic variables. SRS: open soil respiration system with 6 chambers for the soil surface $CO_2$ flux measurements ($F_{sch}$) and 1 chamber for the trenched plots measurements ($F_{tr}$). Gradient system: $CO_2$ sensors inserted into the soil for measuring soil $CO_2$ concentration and calculating the following fluxes: $CO_2$ flux at the soil surface ($F_{sbg}$), below-ground $CO_2$ flux between layer 2 ($L_2$) and layer 1 ($L_1$) ($F_{bg1}$), below-ground $CO_2$ flux between layer 3 ($L_3$) and layer 2 ($F_{bg2}$)

years this grassland can turn into a net carbon source (Nagy et al. 2007), annual sums of net ecosystem exchange (NEE) were ranging between −171 and +106 g C m$^{-2}$ years$^{-1}$ (Pintér et al. 2010).

The EC system consists of a CSAT3 sonic anemometer (Campbell Scientific, USA) and a Li-7500 (Licor Inc, USA) open-path infra-red gas analyser (IRGA), both connected to a CR5000 data logger (Campbell Scientific, USA) via an SDM (synchronous device for measurement) interface. Additional measurements used in this study were: air temperature and relative humidity (HMP35AC, Vaisala, Finland), precipitation (ARG 100 rain gauge, Campbell, UK), global radiation (dual pyranometer, Schenk, Austria) incoming and reflected photosynthetically active radiation (SKP215, Campbell, UK), volumetric soil moisture content (CS616, Campbell, UK) and soil temperature (105 T, Campbell, UK). These measurements were performed as described in Nagy et al. (2007) and Pintér et al. (2010). Fluxes of sensible and latent heat and $CO_2$ were processed using an IDL program after Barcza et al. (2003) adopting the CarboEurope IP methodology. For a detailed description of data processing and gap-filling see Nagy et al. (2007) and Farkas et al. (2011).

*Soil respiration system*

The automated soil respiration system was set up in July 2009. It was upgraded from the 4 chamber to a 10 chamber version in July 2011. The measurement principle is an open dynamic system consisting of an SBA-4 infrared gas analyser (PPSystems, UK), pumps, flow meters (D6F-01A1-110, Omron Co., Japan), electro-magnetic valves, and PVC/metal soil chambers. The chambers were 10.4 cm high with a diameter of 5 cm, covering a soil surface area of approximately 19.6 cm$^2$. The flow rate through the chambers was 300 ml min$^{-1}$, which means that the chamber volume is renewed every 40 s. The PVC chambers were enclosed in a white metal cylinder with 2 mm airspace in between to stabilize the chamber and to prevent warming by direct radiation. Four vent holes with a total area of 0.95 cm$^2$ were drilled in the top of the chambers. Vent holes also served to allow precipitation to drip into the chambers. The system causes minor disturbance in the soil structure and the spatial structure of the vegetation. It is applicable without cutting the leaves/shoots of the plants, so it is not disturbing transport

processes (phloem and xylem) taking place within the plant stems and roots. It is suitable for continuous, long-term unattended measurements of soil $CO_2$ efflux and has been used in previous experiments (Nagy et al. 2011). The soil respiration chambers contained no standing aboveground plant material.

After each hour of operation, the system was kept idle for the following hour. Six chambers were used to monitor the total surface $CO_2$ efflux ($F_{sch}$) and one chamber for measuring the $CO_2$ efflux of trenched plots ($F_{tr}$). This chamber was moved every 2 weeks among the 4 trenched plots, which were installed in 2010. Plastic tubes were used to exclude roots and root-associated microorganisms in these plots. Soil cores (160 mm diameter, 800 mm deep) were drilled and roots were removed from the soil. The soil was put back into the tubes layer by layer. We started our measurements several months after the installation to avoid artefacts from this disturbance. These plots were only used as a standard for the absence of plant physiological effects.

Data of the six chambers ($F_{sch}$) were averaged before analysis. As $F_{tr}$ was measured by only one chamber, but at least twice in one measurement cycle (half an hour), these data were also averaged. Individual measurements were eliminated when the residual of an individual data point was outside the range of the mean±three times the standard deviation of the values in a 21-point moving window centered at this data point.

The system was tested on a calibration tank (CzechGlobe, Brno, Czech Republic) against known fluxes ($F_{sch}=0.98 \times F_{cal}$, r$^2$=0.92, $n$=86) and it was also compared to a LI-6400 system at the study site ($F_{sch}=0.92 \times F_{LI6400}$, r$^2$=0.92, $n$=36).

*Gradient method*

The soil $CO_2$ concentration sensors (gradient system) were installed in June 2009. Three GMP343 (Vaisala, Finland) IRGAs were inserted into the soil at depths of 5, 12 and 35 cm, respectively. They were installed in a distance of about 3 m from the eddy station and within 1–2 m from the soil respiration chambers. The sensors were sampled by the CR5000 data logger (also controlling EC measurements) at 10 s intervals and averaged in half-hourly intervals.

The $CO_2$ fluxes measured by the gradient system were compared to those measured by the soil respiration

system. Good agreement was found between the two methods ($F_{sbg}=0.9334\times F_{sch}$, $r^2=0.61$, $n=3292$).

$CO_2$ fluxes ($F_{sbg}$, $F_{bg1}$, $F_{bg2}$) were calculated according to Moldrup and Olesen (2000) and Davidson et al. (2006a). The water retention curve characteristics in the different layers of the investigated soil were taken from a previous study on the water cycle at the study site (Hagyó 2010). $CO_2$ productions in the different layers were calculated as the difference between the incoming and outgoing $CO_2$ fluxes considering the changes of the $CO_2$ concentrations in the given layer. For a detailed description of the calculations see the Online Resource.

Ancillary measurements

Soil temperatures and volumetric soil water contents were measured at two different depths (5 cm and 30 cm) by the EC system. In order to infer the temperature and soil water content of the intermediate soil layer ($L_2$), a linear temperature change between the top soil layer ($L_1$) and the one at 30 cm depth ($L_2$) was assumed.

Broadband Normalized Difference Vegetation Index (NDVI) values were calculated using the incoming and reflected global and photosynthetically active radiation data according to Wang et al. (2004). Daily maximum radiation was used to calculate the daily NDVI values and running average (1 week window size) of these daily NDVI values were then calculated and used for the analysis.

Soil pH was determined with the KCl method. Soil bulk density was measured using the volumetric core method at 10 cm depth intervals down to 80 cm. Soil texture was determined according to the Hungarian Standard (MSZ-08-0205:1978). Total organic carbon content (TOC) of the samples was determined by sulfochromic oxidation, total nitrogen content (TN) was determined by the Kjeldahl method (Sparks et al. 1996).

Soil respiration models

Three different soil respiration models were used during the data processing to describe the response of the different $CO_2$ fluxes and $CO_2$ production rates to the main abiotic and biotic drivers.

In the Lloyd-Taylor (1994) model (model 1) soil temperature is the only driving variable

$$F = a \times e^{b \times \left(\frac{1}{56.02} - \frac{1}{T_s - 227.13}\right)} \tag{1}$$

where F is the soil $CO_2$ flux ($\mu mol\ CO_2\ m^{-2}\ s^{-1}$), $T_s$ is the soil temperature at 5 cm in Kelvin, $a$ and $b$ are the model parameters.

Model 2 additionally includes SWC (Balogh et al. 2011):

$$F = a \times e^{b \times \left(\frac{1}{56.02} - \frac{1}{T_s - 227.13}\right) + \left[-0.5 \times \left[\ln\left(\frac{SWC}{c}\right)\right]^2\right]} \tag{2}$$

where $T_s$ is the soil temperature at 5 cm in Kelvin, SWC is the volumetric soil water content (%) and $a$, $b$ and $c$ are the model parameters.

Model 3 extended model 2 by adding NDVI (see Section 2.4) as a driving variable:

$$F = a \times e^{d \times NDVI + b \times \left(\frac{1}{56.02} - \frac{1}{T_s - 227.13}\right) + \left[-0.5 \times \left[\ln\left(\frac{SWC}{c}\right)\right]^2\right]} \tag{3}$$
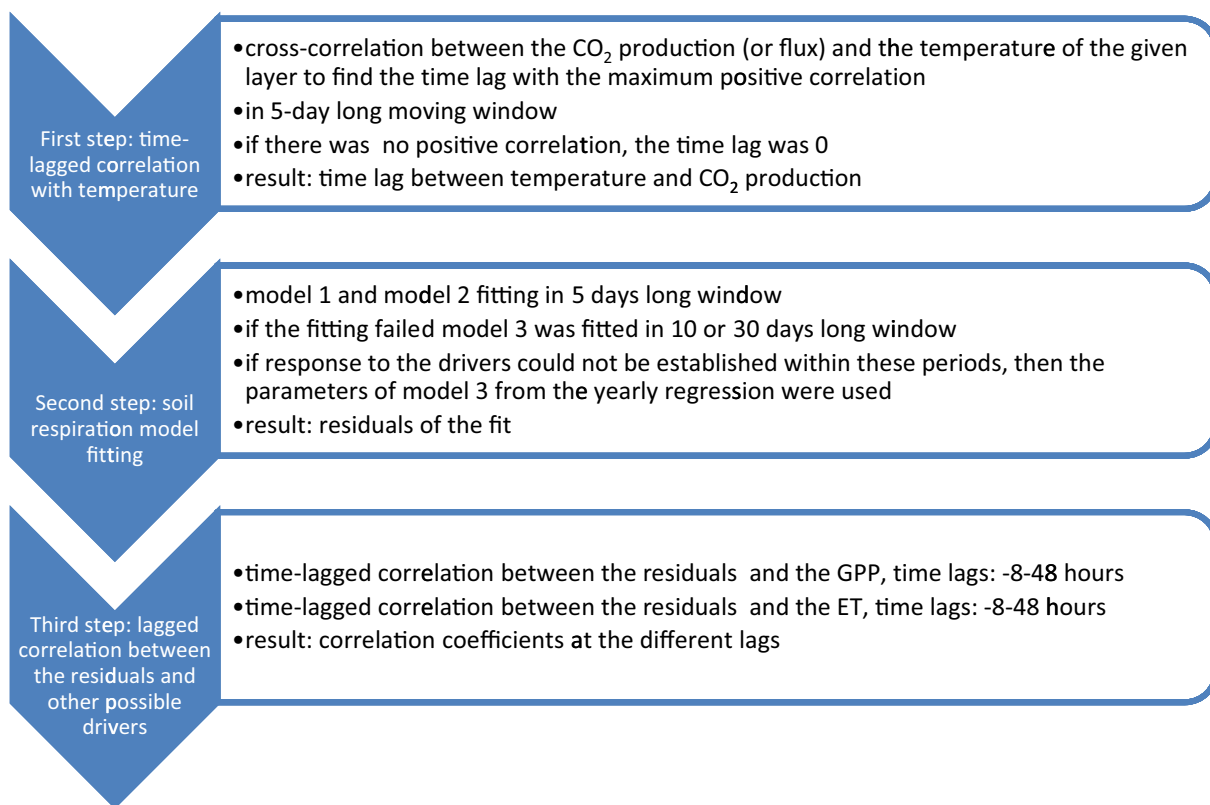
where $T_s$ is the soil temperature at 5 cm in Kelvin, SWC is the volumetric soil water content (%), NDVI is the normalized difference vegetation index and $a$, $b$, $c$ and $d$ are the model parameters.

Nonlinear least-squares fitting was done with Sigmaplot 8.0 (SPSS Inc.) and IDL (ITT Visual Solutions, USA).

Time-series analyses of $CO_2$ productions and fluxes

After calculating the $CO_2$ production rates in the different soil layers we removed the effect of the drivers by subtracting the output of the above described three models from the $CO_2$ production rates and analysed the residuals from each model to infer the effects of additional, possibly important drivers. The same analysis was done on the $CO_2$ efflux rates. The model selection procedure was governed by the dictum to use as low a number of predictors as necessary to still obtain a significant model fit.

The flowchart in Fig. 2 illustrates the main steps of the analysis. In the first step we used lagged cross-correlation to find the time lag with the temperature, as a phase shift between the measured temperature and $CO_2$ efflux was often detected (Pavelka et al. 2007; Ruehr et al. 2009). As it is proposed that the time lag between the temperature measured in the upper layer of the soil and the $CO_2$ production could not be longer than a few hours (Ruehr et al. 2009), we used a 0–6 h time lag

- cross-correlation between the $CO_2$ production (or flux) and the temperature of the given layer to find the time lag with the maximum positive correlation
- in 5-day long moving window
- if there was no positive correlation, the time lag was 0
- result: time lag between temperature and $CO_2$ production

**First step: time-lagged correlation with temperature**

- model 1 and model 2 fitting in 5 days long window
- if the fitting failed model 3 was fitted in 10 or 30 days long window
- if response to the drivers could not be established within these periods, then the parameters of model 3 from the yearly regression were used
- result: residuals of the fit

**Second step: soil respiration model fitting**

- time-lagged correlation between the residuals and the GPP, time lags: -8-48 hours
- time-lagged correlation between the residuals and the ET, time lags: -8-48 hours
- result: correlation coefficients at the different lags

**Third step: lagged correlation between the residuals and other possible drivers**

**Fig. 2** Flowchart of the data analyses steps

window in our analysis. The time lag within this interval with the correlation maximum was chosen for the next step, using zero lag if no positive correlation was found. We used a 5-day moving window approach.

In the second step we fitted the soil respiration models to the measured $CO_2$ fluxes and $CO_2$ production rates. Model 1 (Eq. 1) and model 2 (Eq. 2) were used first in 5-day long moving window. The model with higher $r^2$ was used. The $r^2$ was calculated as: $r^2=1-$(residual sum of squares/total sum of squares).

If the fit failed (i.e., either $r^2$ or the parameters were not significantly different from zero), model 3 was applied with moving window of 10 days, which—if the fit failed again—was increased to 30 days. If the response to the drivers could not be established in the given periods (5, 10, or 30 days), then the parameters of model 3 fitted to the whole dataset were used to calculate the residuals of the fit. The number of cases (days) falling into the different categories are given in the Online Resource.

We assumed that the remaining variance after subtracting the effects of $T_s$, SWC and NDVI could be attributed to the additional drivers, GPP and ET at the diel timescale. This correlation analysis was performed on the whole dataset.

The residuals were used in the last step (Fig. 2) to calculate the time-lagged correlation between the residuals and ET and between the residuals and GPP within a time-lag window between −8 and 48 h.

Data processing was done in IDL (ITT Visual Solutions, USA).

**Results**

Meteorological conditions

The study period of 16 months was dry with 520 mm precipitation in total, which is less than the average annual precipitation. The moisture content of the deeper soil layer was usually lower than that of the upper layer

(Fig. 3). This phenomenon clearly shows that there was not enough precipitation to replenish the deeper soil layers, even during the winter. The seasonal change of the NDVI was reflected in the seasonal change of NEE and GPP (Fig. 4a, b). The highest NDVI values were observed at the beginning of June 2012, while the lowest occurred during a drought period at the end of July 2012.

### Annual course of $CO_2$ fluxes and production in the soil

Annual courses of $CO_2$ and $H_2O$ fluxes were determined by the main drivers (Figs. 3 and 4). The effect of the long, dry autumn of 2011 is shown in Fig. 4 as a continuous decrease in all gas exchange rates from the end of August 2011 until the end of the year. Both $CO_2$ uptake and $CO_2$ efflux rates were low until the beginning of March 2012. The highest activity was detected in May and June 2012 at time of peak biomass (Fig. 3c).

Two active periods could be distinguished in 2012 (Fig. 4b): from April to June and in October. There was an extensive drought period in-between, during which the decrease in respiration activity was less pronounced than that in GPP.

Sudden declines in below-ground fluxes (Fig. 4f, g) were observed several times during the study period. These cases, when flux rates can drop to zero (e.g. $F_{bg2}$, in May and June 2012), were observed during precipitation events and resulted in large variances in the below-ground $CO_2$ fluxes within a short period of time.

The mean daily $CO_2$ production rates are shown in Fig. 4h. The upper soil layer ($L_1$) had the highest $CO_2$ production during the study period, even during winter, and during the drought in autumn 2011. The minimum and maximum contributions of the different layers to the total daily $CO_2$ production rates were 30–79 %, 18–43 % and 2–26 % with averages 54, 33 and 13 % in $L_1$, $L_2$ and $L_3$, respectively.
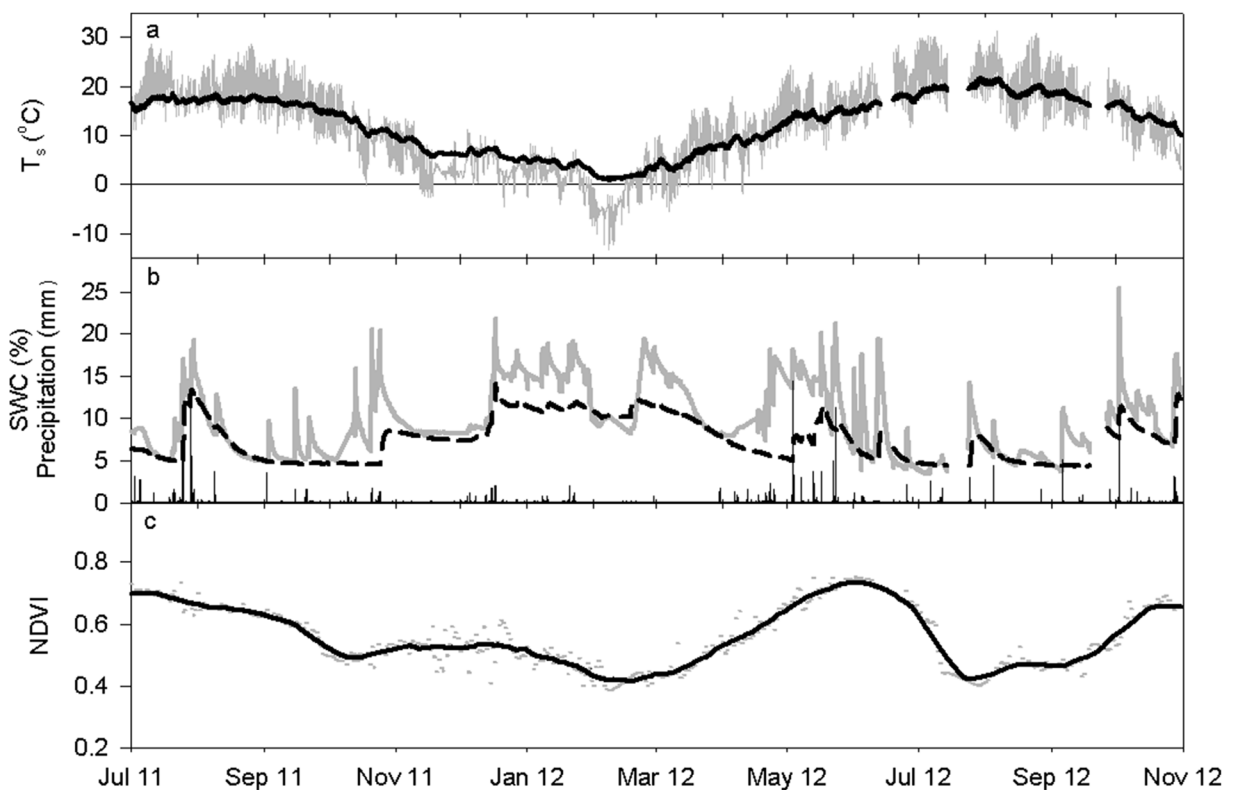


**Fig. 3** Half-hourly **a** soil temperature ($T_s$) at 5 cm (*grey line*) and at 30 cm depth (*black line*), **b** precipitation (*bars*) and volumetric soil water content (SWC) at 5 cm (*grey line*) and at 30 cm depth (*black line*) and **c** broadband NDVI values at maximum radiation (*grey dots*) and their moving average (*black line*, window size: 10 days) during the study period (1/7/2011–30/10/2012) at the Bugac site
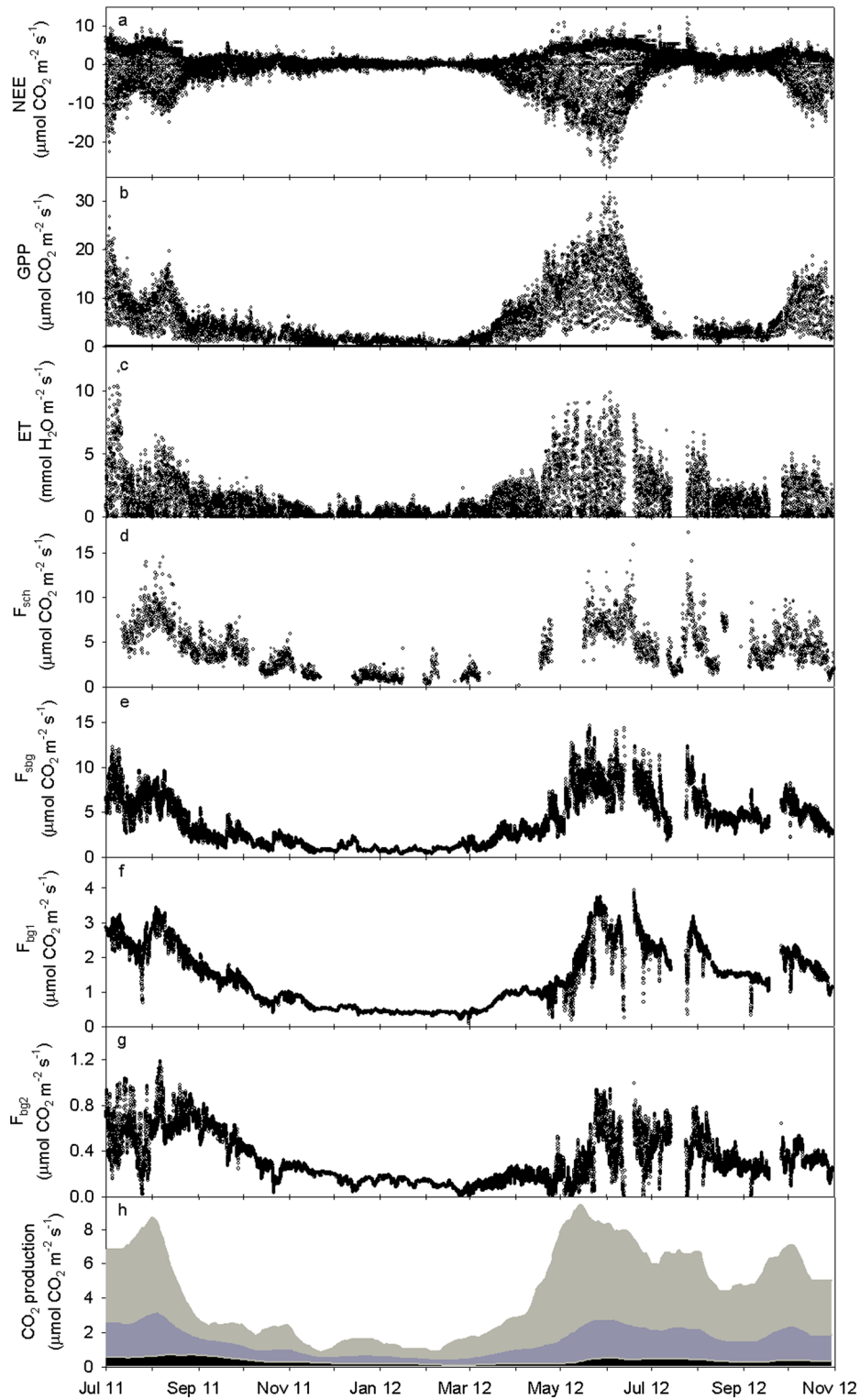
**Fig. 4** Seasonal variations of the different half-hourly fluxes as measured by the eddy system (**a-c**: NEE, GPP, ET), the soil respiration system (**d**: $F_{sch}$) and the gradient system (**e-g**: $F_{sbg}$, $F_{bg1}$, $F_{bg2}$), and (**h**) mean daily $CO_2$ production in the different layers during the study period at Bugac (*grey*: layer 1+2+3, *dark grey*: layer 2+3, *black*: layer 3) during the study period (1/7/2011–30/10/2012) at the Bugac site

Diel courses of gas exchange

$CO_2$ production was often lower during daytime than during nighttime. In order to investigate this phenomenon, half-hourly averages were selected when NDVI values exceeded 0.68 (Fig. 3c) during the 16 months study period in 2011 and 2012. This selection led to a subset of 58 days. Average diel courses of $CO_2$ efflux and production rates, ET, GPP and $T_s$ were then computed from the selected data (Fig. 5).

The average $CO_2$ production within $L_1$ (the dominant layer) was lower during much of the day than during night-time on the selected days. $T_s$ of the layer, however, followed a different course, peaking during daytime in the late afternoon (Fig. 5a). The average daytime evapotranspiration was high on the selected days (Fig. 5a).

Figure 5c shows the average $CO_2$ production in the upper layer ($P_{L1}$) as a function of evapotranspiration (ET), while the circle size shows soil temperature. With increasing soil temperatures during the morning and decreasing ones during the night, a counter clockwise hysteresis of $P_{L1}$ was found. $P_{L1}$ started to decrease after a short rising period (until 7 h) despite the increasing temperature. In parallel with the temperature ET was increasing until midday. $P_{L1}$ started to rise only when ET stopped to increase (from 12 h), peaking when ET was close to zero but $T_s$ was still high (20 h). During the night $P_{L1}$ was decreasing again as well as soil temperature. A positive correlation with soil temperature was found during the night and at midday (12–14 h), leading to the observed hysteresis. The minimum $CO_2$ production rate was 21 % lower than the maximum (4.56 and 5.78 μmol $CO_2$ m$^{-2}$ s$^{-1}$, respectively), although the maximum was measured at the lower soil temperature (21.3 and 18.7 °C).

Time lag between transpiration, C uptake, environmental conditions and respiration losses

*Summary of model results and residual analysis*

In the case of $F_{sch}$ the Lloyd-Taylor model (model 1, $r^2$ = 0.43) gave lower goodness-of-fit value than the model including the log-normal soil moisture response (model 2, $r^2$=0.56). The incorporation of NDVI into the soil respiration model improved $r^2$ further by 13 % (model 3, $r^2$=0.689) (Table 2).

The average soil $CO_2$ efflux measured at the surface ($F_{sch}$) showed no correlation with average ET nor with the average soil temperature in the active period when NDVI values exceeded 0.68, even when a time lag of up to 5 h was considered, while fluxes from the vegetation removal treatment ($F_{tr}$) showed best correlation with temperature at 0 h time lag (data not shown). We however had expected that the effect of ET on $P_{L1}$ should also be found in the surface soil $CO_2$ efflux, therefore we asked the question whether this effect can be seen in the residuals. We used model 3 to remove the effect of the main abiotic drivers from the whole dataset. For $F_{sch}$ residuals a significant negative correlation was found with ET during the active periods, selected by high NDVI values (≥0.68). Contrastingly, no correlation was found between $F_{tr}$ residuals and ET for the same period.

To quantify the effect of ET on soil respiration rates, standardized flux residuals were plotted as a function of ET. At low ET values, $F_{sch}$ was 5 % higher than predicted by the model. At high ET rates, the measured $F_{sch}$ was significantly lower than predicted (−10 to −20 % at ET >6 mmol $H_2O$ m$^{-2}$ s$^{-1}$). Overall, the difference between the standardized residuals at low and high evapotranspiration rates was about 0.2, which means a 20 % difference compared to the measured $CO_2$ effluxes (Fig. 6a).

*Results of time-series analyses*

Correlations between $F_{sch}$, $P_{L1-3}$ and abiotic ($T_s$, SWC) and biotic drivers (ET, GPP) were further analysed with time-series analyses of the whole dataset in order to reveal the detailed diel and seasonal correlations.

Time lagged correlations between $F_{sch}$, $P_{L1-3}$ and $T_s$ were calculated in the first step of our analyses (cf. Fig. 2) using moving windows of 5 days length. No consistent time lag was found between the two variables. In the case of $F_{sch}$ the correlation coefficient was statistically significant in 158 out of the 345 cases (days), with a zero lag being the most frequent time lag (92 cases or 58 % of these cases). Cases with significant correlations were uniformly distributed over the study period with no seasonal preference (data not shown).

Time lagged correlation was further analysed both with ET and GPP for the full study period. Residuals were calculated after subtracting the main effects of soil temperature, soil water content and NDVI (Fig. 2) from $F_{sch}$ and $P_{L1-3}$ rates. These residuals were then correlated with ET and GPP. As the time lags of the significant correlations were not normally distributed, we calculated the mode of the time lags for $F_{sch}$ and the $CO_2$ production in the different layers.
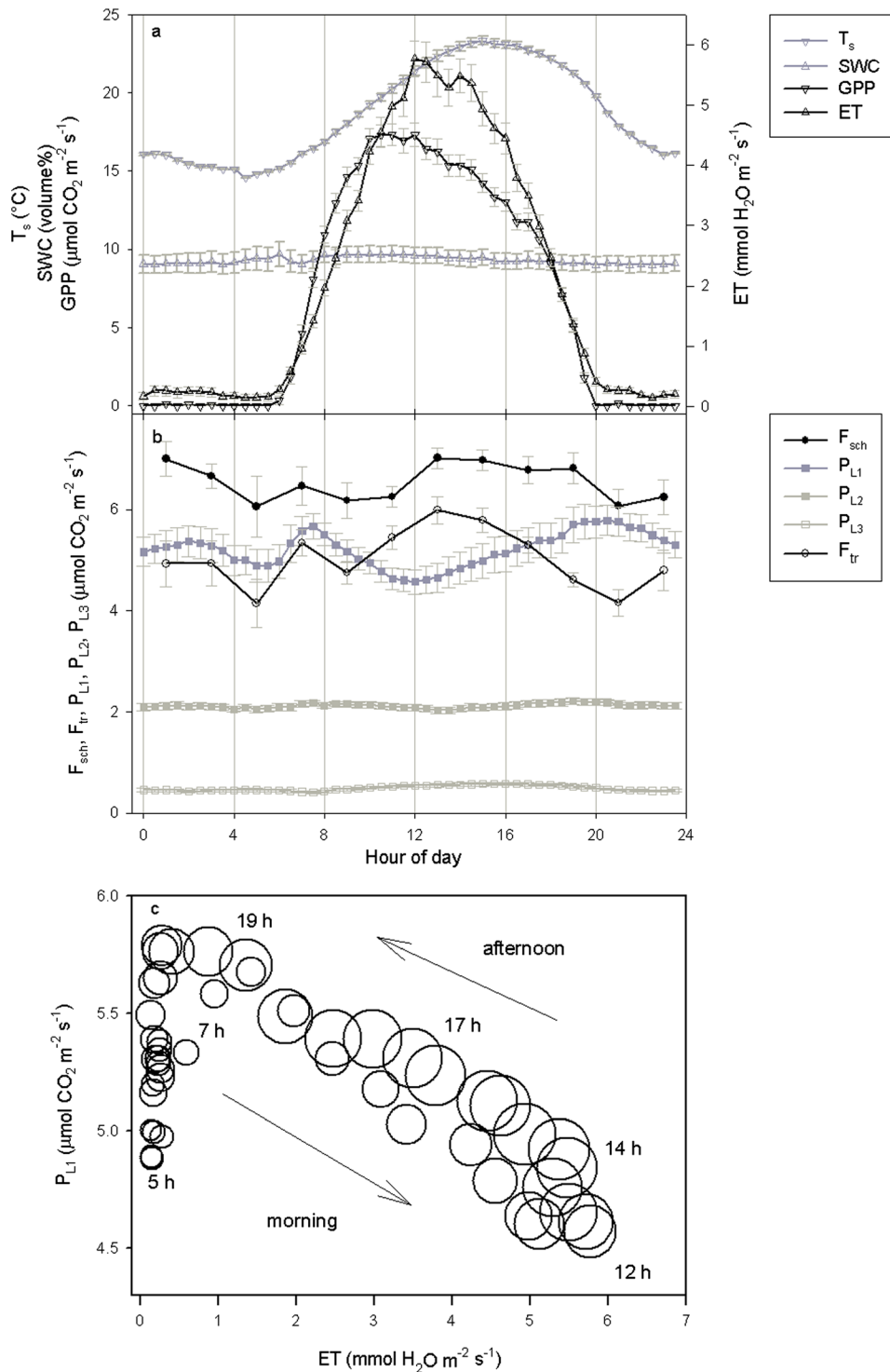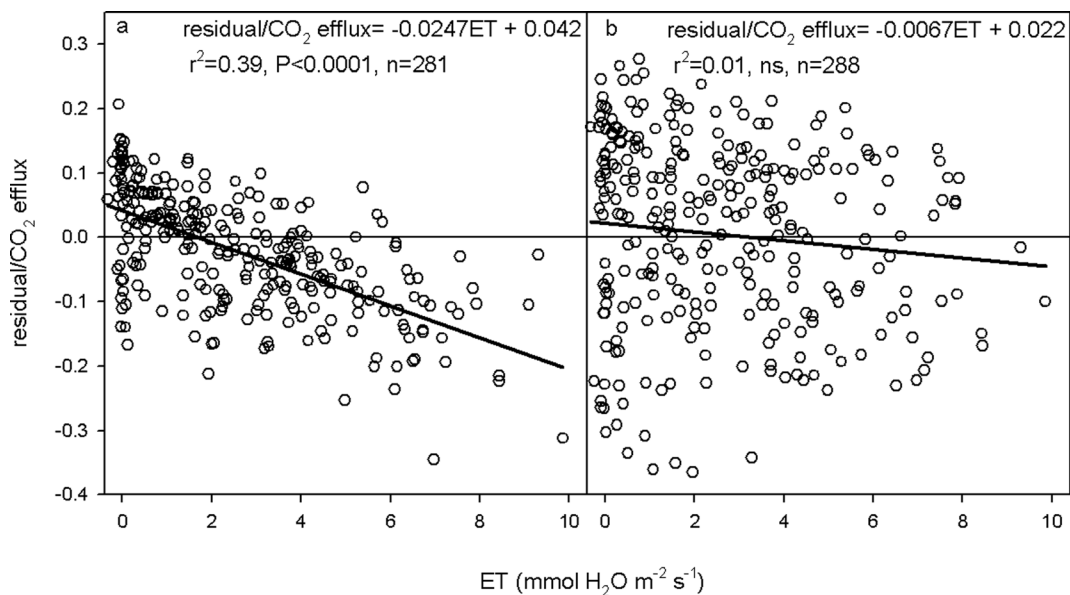
Fig. 5  a Average diel courses of soil temperature at 5 cm ($T_s$), soil moisture at 5 cm (SWC), gross primary production (GPP) and evapotranspiration (ET) in the active period (NDVI≥0.68) in July-August 2011 and in May-June 2012 at the Bugac site. b Average diel courses of total soil $CO_2$ efflux ($F_{sch}$), $CO_2$ efflux of trenched plots ($F_{tr}$) and $CO_2$ production of the three soil layer ($P_{L1}$, $P_{L2}$, $P_{L3}$) in the same period. c Average $P_{L1}$ as a function of average ET in the same period. The size of the *circles* shows the soil temperature (range: 14.6–23.3 °C). Data of 58 days were averaged, with error bars showing the standard error

**Table 2** $r^2$ values, number of data points (N), coefficients after fitting model 1, 2, 3 (Eq. 1–3) to half-hourly average soil surface $CO_2$ fluxes ($F_{sch}$, $F_{tr}$), below-ground fluxes ($F_{sbg}$, $F_{bg1}$, $F_{bg2}$) and $CO_2$ production rates ($P_{L1}$, $P_{L2}$, $P_{L3}$) of the full study period. Statistical significance levels of the coefficients and model fitting were $P<0.0001$ in all cases

| | $r^2$ | N | a | b | c | d |
|---|---|---|---|---|---|---|
| **Model 1** | | | | | | |
| $F = a \times e^{b \times \left(\frac{1}{56.02} - \frac{1}{T_s - 227.13}\right)}$ | | | | | | |
| **$F_{sch}$** | **0.431** | 3590 | 2.53 | 161.55 | – | – |
| $F_{tr}$ | 0.5 | 3349 | 1.89 | 194.96 | – | – |
| $F_{sbg}$ | 0.54 | 22032 | 2.21 | 246.6 | – | – |
| $F_{bg1}$ | 0.68 | 22032 | 0.99 | 236.2 | – | – |
| $F_{bg2}$ | 0.19 | 22020 | 0.15 | 242.01 | – | – |
| $P_{L1}$ | 0.38 | 21807 | 0.76 | 273.4 | – | – |
| $P_{L2}$ | 0.67 | 21999 | 0.72 | 262.9 | – | – |
| $P_{L3}$ | 0.35 | 21954 | 0.17 | 281.07 | – | – |
| **Model 2** | | | | | | |
| $F = a \times e^{b \times \left(\frac{1}{56.02} - \frac{1}{T_s - 227.13}\right)} + \left[-0.5 \times \left[\ln\left(\frac{SWC}{c}\right)\right]^2\right]$ | | | | | | |
| **$F_{sch}$** | **0.555** | 3544 | 2.99 | 208.05 | 12.43 | – |
| $F_{tr}$ | 0.479 | 3349 | 2.17 | 195.76 | 13.08 | – |
| $F_{sbg}$ | 0.58 | 22032 | 2.62 | 308.1 | 14.34 | – |
| $F_{bg1}$ | 0.7 | 22032 | 1.08 | 233.3 | 8.03 | – |
| $F_{bg2}$ | 0.49 | 22020 | 0.303 | 189.19 | 6.08 | – |
| $P_{L1}$ | 0.48 | 21807 | 1.85 | 418.39 | 31.7 | – |
| $P_{L2}$ | 0.69 | 21999 | 0.79 | 297.9 | 10.74 | – |
| $P_{L3}$ | 0.505 | 21954 | 0.26 | 279.16 | 7.8 | – |
| **Model 3** | | | | | | |
| $F = a \times e^{d \times NDVI + b \times \left(\frac{1}{56.02} - \frac{1}{T_s - 227.13}\right)} + \left[-0.5 \times \left[\ln\left(\frac{SWC}{c}\right)\right]^2\right]$ | | | | | | |
| **$F_{sch}$** | **0.689** | 3544 | 0.58 | 177.65 | 11.85 | 2.93 |
| $F_{tr}$ | 0.555 | 3349 | 0.53 | 169.57 | 12.76 | 2.5 |
| $F_{sbg}$ | 0.665 | 22032 | 0.383 | 231.23 | 12.33 | 3.42 |
| $F_{bg1}$ | 0.812 | 22032 | 0.258 | 181.46 | 6.95 | 2.66 |
| $F_{bg2}$ | 0.58 | 22030 | 0.083 | 268.17 | 6.31 | 1.98 |
| $P_{L1}$ | 0.495 | 21184 | 0.38 | 216.67 | 14.79 | 3.12 |
| $P_{L2}$ | 0.751 | 21185 | 0.224 | 234.25 | 9.69 | 2.48 |
| $P_{L3}$ | 0.58 | 21184 | 0.085 | 315.07 | 7.54 | 1.84 |

**Fig. 6** Standardized residuals of **a** surface $CO_2$ efflux ($F_{sch}$) and **b** trenched plots without roots ($F_{tr}$) as a function of ET values in the active periods with NDVI ≥0.68. The linear regressions are shown (solid line)

Strong negative correlations between the residuals and ET were found mostly between −2 and 5 h time lag in the upper two layers, but with longer time lags in the third layer (Online Resource Fig. 2 b–d). Approximately 12–16 h after the negative correlation peak there was a positive correlation in all cases. The annual course of the significant correlations shows that the time lag of the negative correlations slightly changes during the year (Online Resource Fig. 2). There was no clear diel pattern during winter. The modes of time lags of the significant negative correlations for $F_{sch}$, $P_{L1}$, $P_{L2}$ and $P_{L3}$, respectively were at 1.5, 0.5, 0.5, 4.5 h.

In the case of the GPP we assumed that the positive correlation maximum represents the connection between GPP and $CO_2$ production. Positive significant correlations could be found during the whole study period, but the correlation coefficient was lower than that with ET (Online Resource Fig. 2 e–h). The modes of the time lags of the significant positive correlations for $F_{sch}$, $P_{L1}$, $P_{L2}$ and $P_{L3}$, respectively were at 15, 11, 18, 20 h.

## Discussion

### Annual course of $CO_2$ fluxes and production in the soil

The seasonal courses of the $CO_2$ fluxes followed the changes of the main environmental drivers, as temperature (as well as incoming radiation) and the amount of soil

water available to plants. There were differences between the two autumns studied: the second half of 2011 was very dry, the soil $CO_2$ production rates in autumn 2012 were two times the rates observed in autumn 2011 (Fig. 4). Significant rain events affected the belowground $CO_2$ fluxes negatively, especially the below-ground fluxes (Fig. 4). The observed decline (even down to zero) in these fluxes was mainly caused by the indirect effect of precipitation: the increasing $CO_2$ concentration due to the enhanced respiratory activity on excess moisture in the upper soil layers decreased, or even reversed the normal $CO_2$ gradient within the soil (Nagy et al. 2011).

The distribution of the $CO_2$ production rates along the three soil layers corresponded well with our expectations. It was expected that the upper layer would be the most significant in contributing to total $CO_2$ efflux (Davidson et al. 2006a; Verma and Kelleners 2012), since it contains the majority of active roots and associated microbial communities (Subke and Bahn 2010) as well as the majority of the fresh SOM. In spite of the highly variable water supply, the upper layer was the main contributor to the total $CO_2$ efflux even under drought conditions (Fig. 4).

### Diel courses of gas exchange

$CO_2$ production rates were often found to be higher during the night than during daytime (Fig. 5a) in the active periods. Several factors that could be the reason

for this phenomenon were considered. Since highest $CO_2$ concentrations up to 1400 ppm at 10 cm above ground level are found during nights with no wind, or low wind velocity, the question is whether these high concentrations in the air are actually rather a result of $CO_2$ advection from surrounding areas which would then be erroneously interpreted as higher apparent productivity in the soil. If this were the case, then we would expect an apparently positive correlation between calculated soil $CO_2$ production (as a direct function of measured $CO_2$ concentration in the soil), and soil temperature, based on the fact that soils tend to cool less under calm and low wind speed conditions, and consequently temperature stays highest in these periods. Our data, however, show the opposite: a significantly negative correlation between $P_{L1}$ and $CO_2$ concentration at 10 cm during nights of the active period. This finding also excludes the potential interpretation that soil temperatures remain warmer during calm nights (which would result in increased $P_{L1}$) than during more turbulent nights.

Alternatively, the increase of both autotrophic and heterotrophic respiration due to water redistribution from deeper layers to the dry surface soil layer (Carbone et al. 2008; Ruehr et al. 2009), could explain the higher nighttime production. However, the water content of the upper layers showed no significant changes during the day (0.7 % on average during the selected period with NDVI ≥0.68) as would be required to maintain this hypothesis. Another explanation could be increased water availability during the night and especially in the early morning when the surface water content can be increased by dew formation. But this phenomenon possibly only affects the uppermost layer (litter and the surface of the soil) and is unlikely to influence deeper layers.

From this we conclude that it may not be the increase in respiration at night that needs further attention, but the decrease in respiration during the day. It was recently found that transpiration can modify the apparent autotrophic $CO_2$ production by the transport of $CO_2$ in the xylem of trees (Grossiord et al. 2012; Bloemen et al. 2013a, b). Therefore, the transpiration should be considered as a factor potentially affecting apparent soil $CO_2$ production, not only in trees, but also in grasses, herbs and forbes. $CO_2$ produced in the soil that equilibrates with the $CO_2$ in the xylem stream in the roots bypasses the conventional soil chamber measurements, and thus we can hypothesize that a negative correlation

with a short time lag should be found between respiration processes and ET. Our measurements are in agreement with this hypothesis: a negative correlation was found between $P_{L1}$ and ET. $P_{L1}$ was correlated with soil temperature at night and during midday (12–14 h) when ET was almost constant. Contrastingly, during times with little temporal changes in $T_s$ but relevant changes in ET (e.g. during the afternoon, 14–19 h) a negative correlation between $P_{L1}$ and ET led to the hysteresis loop seen in Fig. 5c. These two factors seemed to govern the changes in $P_{L1}$ during the entire day. The short rising period of $P_{L1}$ in the early morning could be attributed to the temperature changes, but when ET became significantly higher (more than 1 mmol $H_2O$ m$^{-2}$ s$^{-1}$) $P_{L1}$ started falling. Another turning point was with decreasing ET during late afternoon: $P_{L1}$ was rising to its maximum after ET started to decline, despite the decreasing temperature. Our results show that $P_{L1}$ was lowered by about 20 % due to the effect of transpiration. No correlation was found between $F_{sch}$ and $T_s$, nor ET. However, $F_{tr}$ was positively correlated with both $T_s$ and ET. This difference indirectly shows the significance of living roots in the soils and their potential to modify soil $CO_2$ efflux via transpiration.

Time lag between evapotranspiration, C uptake, environmental conditions and respiration losses

*Summary of model results and residual analysis*

The Lloyd-Taylor soil respiration model extended by a log-normal function of soil moisture and by an exponential function of NDVI was able to properly describe the response of soil respiration to these drivers at our site. The log-normal shape of soil moisture-respiration response was proposed before (Balogh et al. 2011; Moyano et al. 2013). It originated from the Michaelis-Menten kinetics of the response of respiration to substrate and oxygen availability (Davidson et al. 2012). The incorporation of NDVI into the soil respiration model improved the explanatory power of the model similarly to the findings of Huang and Niu (2012). As the reflectance and greenness of the surface change with the phenological changes of the vegetation, photosynthesis-related vegetation indices can be used to estimate the effect of $CO_2$ uptake on respiration (Huang et al. 2012), or even the ratio of root-derived $CO_2$ in ecosystem respiration (Wang et al. 2010), so it

can be incorporated into soil respiration models (Huang and Niu 2012).

After subtracting the effect of the main drivers by fitting model 3 we found a significant negative correlation between the residuals of the soil respiration rates and ET when NDVI was high. The difference between soil respiration at low and at high transpiration rates could reach as much as 20 % as compared to the measured rates. Similar results were obtained when only the $CO_2$ production of the upper layer was considered (Fig. 5). The effect is not so high as it was found for trees (Aubrey and Teskey 2009), but still it was significant, hence it should be considered in soil $CO_2$ production models. This suggests that calculations and modelling based on daytime measurements in the active periods could significantly underestimate the real $CO_2$ production of the soil.

### Results of time-series analyses

Contrary to the findings of other studies (Davidson et al. 2006b; Vargas et al. 2010), there was no consistent time lag between soil temperature and soil $CO_2$ efflux, neither at higher, nor at lower soil water contents (data not shown). The most frequent time lag with significant correlation between soil temperature and soil $CO_2$ efflux ($F_{sch}$) was 0 h and the average lag time of significant correlations was 1.15 h. These time lags are in good agreement with the $CO_2$ production rates, which can be explained by the upper layer (0–8 cm) being the main contributor to the total $CO_2$ efflux with the calculated diffusion rates.

Several studies (e.g. Moyano et al. 2007; Kuzyakov and Gavrichkova 2010; Hopkins et al. 2013) proposed $CO_2$ uptake (GPP) as a driver of soil (root) respiration, while others (e.g. Aubrey and Teskey 2009; Bloemen et al. 2013a) stated that the transpiration has a major effect on the diel variability of soil $CO_2$ efflux. The daily courses of transpiration and GPP are very similar due to the stomatal co-regulation of both processes (Hetherington and Woodward 2003). Therefore, it could be difficult to separate the two effects. In this study, we found similar time-lagged correlations of $CO_2$ production with ET and GPP, but the correlations were stronger in the case of ET during the whole study period.

The effect of $CO_2$ uptake can be significant according to girdling studies (Högberg et al. 2001; Jones et al. 2009), but it can be assumed that its effect on the diel variability can be less pronounced due to the longer turnover time of soluble carbohydrates compared to diel changes (Högberg et al. 2008). Moreover, starch accumulation during the day ensures the continuous carbohydrate export from leaves to non-photosynthetic tissues at night, avoiding large fluctuations on diel scale (Lu et al. 2005; Mencuccini and Hölttä 2010).

But the effect of ET is expected to be instantly: root water uptake should keep pace with transpiration (Aston and Lawlor 1979), especially in herbaceous plants where the role of capacitance is probably minor as compared to trees (Högberg and Read 2006). In this study, a shorter time lag was found in the response to ET (0.5 h time lag in the upper soil layers) compared to a longer one with GPP (11–18 h in the upper soil layers). The latter corresponds well with an average a time lag of 12.5 h between $CO_2$ uptake and soil respiration found by different studies in grasslands, while this time lag increased to 22 h if only field studies were considered (Kuzyakov and Gavrichkova 2010).

Further, the time lags of the peak correlation changed during the study period. Longer time lags for ET and GPP were obtained in the most active periods for all layers. This can be explained by the fact that transport routes of carbon and water get longer as the shoot and the root systems become longer in the course of the season (Mencuccini and Hölttä 2010). The same effect could be important in deeper layers: the longer the route within the plant, the longer the time lags between the physiological processes.
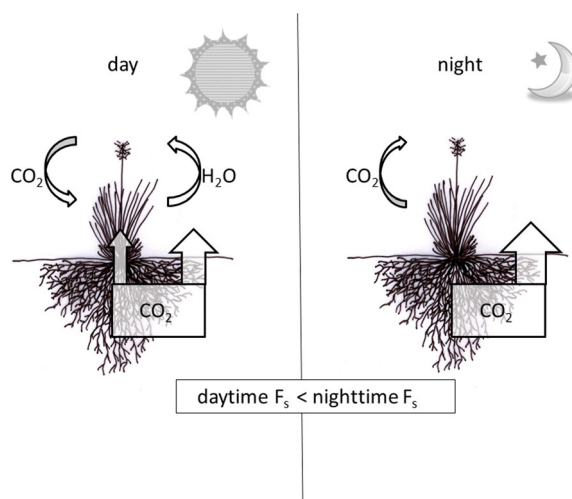


**Fig. 7** The difference between daytime and nighttime soil respiration processes in grasslands: a significant part of the $CO_2$ produced in the soil could be transported via transpiration stream and assimilated in the plant during daytime

## Implications for soil and ecosystem respiration measurements

According to our results, soil $CO_2$ production could be decreased by 20 % due to the effect of evapotranspiration (Fig. 7) in the active periods. Since manual soil respiration measurements are usually made during daytime due to practical reasons, response functions to environmental drivers derived from these measurements could underestimate the all-day $CO_2$ efflux. Given the amount of $CO_2$ emitted through the soil to the atmosphere is lower during daytime due to the xylem-transported $CO_2$, but does it have any effect on the calculations of ecosystem respiration ($R_{eco}$)? Daytime $R_{eco}$ estimations are usually based on the temperature response observed at night (Reichstein et al. 2005), thus when the soil $CO_2$ efflux to the atmosphere has shown to be higher at our site. However we should consider that the transpiration stream does not affect the amount of $CO_2$ produced under the surface, our results only suggest that the transport route could be different at daytime and nighttime. Therefore it can be assumed that this phenomenon has no influence on GPP estimations in grasslands. Bloemen et al. (2013b) found that most of the xylem-transported $CO_2$ was respired to the atmosphere through stem and branch efflux in trees. However, the important difference between herbaceous plants and trees in this respect is that the transport route is shorter and that the xylem sap $CO_2$ transport happens in the vicinity of the photosynthetic tissues. Therefore the re-fixation of the xylem-transported $CO_2$ is more likely in herbaceous plants.

Our results showed a nice example how the different gas fluxes are tightly coupled in the soil-vegetation-atmosphere system. Soil respiration models considering this phenomenon could be able to explain a large part of diel variation and improve the goodness of annual sum estimations and GPP partitions.

## Conclusions

Three automated techniques of $CO_2$ gas exchange measurements were used to quantify the effects of principal biotic and abiotic factors on soil $CO_2$ production on different (from diel to annual) timescales. We found that besides temperature and soil moisture, transpiration was controlling the diel course of the $CO_2$ production. After subtracting the effects of the main abiotic drivers we

found strong negative correlations between evapotranspiration and soil $CO_2$ production rates, and less strong, but still significant positive correlations between gross $CO_2$ uptake and soil $CO_2$ production. Since our results suggest that the daytime $CO_2$ production measurements in grasslands could be underestimated due to the $CO_2$ transport in the xylem, our findings strongly suggest that the effect of transpiration should be considered both in soil respiration models and in field measurement protocols.

Our results provide further evidence of a potential hidden $CO_2$ transport within the plants, which is not measured by traditional $CO_2$ gas exchange techniques. Estimations of soil $CO_2$ production and GPP would hence benefit from explicit consideration of this phenomenon.

## References

Aston MJ, Lawlor DW (1979) The relationship between transpiration, root water uptake and leaf water potential. J Exp Bot 30:169–181

Aubrey DP, Teskey RO (2009) Root-derived $CO_2$ efflux via xylem stream rivals soil $CO_2$ efflux. New Phytol 184:35–40. doi:10.1111/j.1469-8137.2009.02971.x

Balogh J, Pintér K, Fóti S et al (2011) Dependence of soil respiration on soil moisture, clay content, soil organic matter, and $CO_2$ uptake in dry grasslands. Soil Biol Biochem 43:1006–1013. doi:10.1016/j.soilbio.2011.01.017

Barcza Z, Haszpra L, Kondo H (2003) Carbon exchange of grass in Hungary. Tellus B 187–196

Bekku Y, Sakata T, Tanaka T, Nakano T (2011) Midday depression of tree root respiration in relation to leaf transpiration. Ecol Res 26:791–799. doi:10.1007/s11284-011-0838-z

Blagodatsky S, Smith P (2012) Soil physics meets soil biology: towards better mechanistic prediction of greenhouse gas emissions from soil. Soil Biol Biochem 47:78–92. doi:10.1016/j.soilbio.2011.12.015

Bloemen J, McGuire MA, Aubrey DP et al (2013a) Transport of root-respired $CO_2$ via the transpiration stream affects aboveground carbon assimilation and $CO_2$ efflux in trees. New Phytol 197:555–65. doi:10.1111/j.1469-8137.2012.04366.x

Bloemen J, McGuire MA, Aubrey DP et al (2013b) Assimilation of xylem-transported $CO_2$ is dependent on transpiration rate

but is small relative to atmospheric fixation. J Exp Bot 64: 2129–38. doi:10.1093/jxb/ert071

Carbone MS, Vargas R (2008) Automated soil respiration measurements: new information, opportunities and challenges. New Phytol 177:297–300. doi:10.1111/j.1469-8137.2007. 02336.x

Carbone MS, Winston GC, Trumbore SE (2008) Soil respiration in perennial grass and shrub ecosystems: linking environmental controls with plant and microbial sources on seasonal and diel timescales. J Geophys Res 113, G02022. doi:10.1029/ 2007JG000611

Davidson E, Savage K, Trumbore S, Borken W (2006a) Vertical partitioning of $CO_2$ production within a temperate forest soil. Glob Chang Biol 12:944–956. doi:10.1111/j.1365-2486. 2006.01142.x

Davidson EA, Janssens IA, Luo Y (2006b) On the variability of respiration in terrestrial ecosystems: moving beyond $Q_{10}$. Glob Chang Biol 12:154–164. doi:10.1111/j.1365-2486. 2005.01065.x

Davidson EA, Samanta S, Caramori SS, Savage K (2012) The Dual Arrhenius and Michaelis-Menten kinetics model for decomposition of soil organic matter at hourly to seasonal time scales. Glob Chang Biol 18:371–384. doi:10.1111/j. 1365-2486.2011.02546.x

Eler K, Plestenjak G, Ferlan M et al (2013) Soil respiration of karst grasslands subjected to woody-plant encroachment. Eur J Soil Sci 64:210–218. doi:10.1111/ejss.12020

Farkas C, Alberti G, Balogh J et al (2011) Methodologies. In: Haszpra L (ed) Atmospheric greenhouse gases: the Hungarian perspective. Springer, New York, pp 65–90

Fóti S, Balogh J, Nagy Z et al (2014) Soil moisture induced changes on fine-scale spatial pattern of soil respiration in a semi-arid sandy grassland. Geoderma 213:245–254. doi:10. 1016/j.geoderma.2013.08.009

Graf A, Weihermüller L, Huisman J et al (2008) Measurement depth effects on the apparent temperature sensitivity of soil respiration in field studies. Biogeosciences 5:1175–1188

Grossiord C, Mareschal L, Epron D (2012) Transpiration alters the contribution of autotrophic and heterotrophic components of soil $CO_2$ efflux. New Phytol 194:647–53. doi:10.1111/j. 1469-8137.2012.04102.x

Hagyó A (2010) Vízforgalom gyep és erdő területeken (Water cycle of grasslands and forests). PhD Thesis, Szent István University, p.129

Hetherington AM, Woodward FI (2003) The role of stomata in sensing and driving environmental change. Nature 424:901–908

Högberg P, Read DJ (2006) Towards a more plant physiological perspective on soil ecology. Trends Ecol Evol 21:548–54. doi:10.1016/j.tree.2006.06.004

Högberg P, Nordgren A, Buchmann N et al (2001) Large-scale forest girdling shows that current photosynthesis drives soil respiration. Nature 411:789–92. doi:10.1038/35081058

Högberg P, Högberg MN, Göttlicher SG et al (2008) High temporal resolution tracing of photosynthate carbon from the tree canopy to forest soil microorganisms. New Phytol 177:220–8. doi:10.1111/j.1469-8137.2007.02238.x

Hopkins F, Gonzalez-Meler MA, Flower CE et al (2013) Ecosystem-level controls on root-rhizosphere respiration. New Phytol 199:339–51

Huang N, Niu Z (2012) Estimating soil respiration using spectral vegetation indices and abiotic factors in irrigated and rainfed agroecosystems. Plant Soil 367:535–550. doi:10.1007/ s11104-012-1488-9

Huang N, Niu Z, Zhan Y et al (2012) Relationships between soil respiration and photosynthesis-related spectral vegetation indices in two cropland ecosystems. Agric For Meteorol 160: 80–89. doi:10.1016/j.agrformet.2012.03.005

Jia B, Zhou G (2009) Integrated diurnal soil respiration model during growing season of a typical temperate steppe: Effects of temperature, soil water content and biomass production. Soil Biol Biochem 41:681–686. doi:10.1016/j.soilbio.2008. 12.030

Jones DL, Nguyen C, Finlay RD (2009) Carbon flow in the rhizosphere: carbon trading at the soil–root interface. Plant Soil 321:5–33. doi:10.1007/s11104-009-9925-0

Kuzyakov Y, Gavrichkova O (2010) Review: time lag between photosynthesis and carbon dioxide efflux from soil: a review of mechanisms and controls. Glob Chang Biol 16:3386–3406. doi:10.1111/j.1365-2486.2010.02179.x

Lellei-Kovács E, Kovács-Láng E, Botta-Dukát Z et al (2011) Thresholds and interactive effects of soil moisture on the temperature response of soil respiration. Eur J Soil Biol 47: 247–255. doi:10.1016/j.ejsobi.2011.05.004

Lloyd J, Taylor J (1994) On the temperature dependence of soil respiration. Funct Ecol 8:315–323

Lu Y, Gehan J, Sharkey T (2005) Daylength and circadian effects on starch degradation and maltose metabolism. Plant Physiol 138:2280–2291. doi:10.1104/pp. 105.061903.2280

Martin JG, Phillips CL, Schmidt A et al (2012) High-frequency analysis of the complex linkage between soil $CO_2$ fluxes, photosynthesis and environmental variables. Tree Physiol 32: 49–64. doi:10.1093/treephys/tpr134

Mencuccini M, Hölttä T (2010) The significance of phloem transport for the speed with which canopy photosynthesis and belowground respiration are linked. New Phytol 185:189–203. doi:10.1111/j.1469-8137.2009.03050.x

Moldrup P, Olesen T (2000) Predicting the gas diffusion coefficient in undisturbed soil from soil water characteristics. Soil Sci Soc Am J 64:94–100

Moyano F, Kutsch W, Schulze E (2007) Response of mycorrhizal, rhizosphere and soil basal respiration to temperature and photosynthesis in a barley field. Soil Biol Biochem 39:843–853. doi:10.1016/j.soilbio.2006.10.001

Moyano FE, Manzoni S, Chenu C (2013) Responses of soil heterotrophic respiration to moisture availability: an exploration of processes and models. Soil Biol Biochem 59:72–85. doi:10.1016/j.soilbio.2013.01.002

Nagy Z, Pintér K, Czóbel S et al (2007) The carbon budget of semi-arid grassland in a wet and a dry year in Hungary. Agric Ecosyst Environ 121:21–29. doi:10.1016/j.agee.2006.12.003

Nagy Z, Pintér K, Pavelka M et al (2011) Carbon balance of surfaces vs. ecosystems: advantages of measuring eddy covariance and soil respiration simultaneously in dry grassland ecosystems. Biogeosciences 8:2523–2534. doi:10.5194/bg-8-2523-2011

Parkin TB, Kaspar TC (2003) Temperature controls on diurnal carbon dioxide flux : implications for estimating soil carbon loss. Soil Sci Soc Am J 67:1763–1772

Pavelka M, Acosta M, Marek MV et al (2007) Dependence of the $Q_{10}$ values on the depth of the soil temperature measuring

point. Plant Soil 292:171–179. doi:10.1007/s11104-007-9213-9

Pintér K, Balogh J, Nagy Z (2010) Ecosystem scale carbon dioxide balance of two grasslands in Hungary under different weather conditions. Acta Biol Hung 61(Suppl):130–5. doi:10.1556/ABiol.61.2010.Suppl.13

Reichstein M, Falge E, Baldocchi D et al (2005) On the separation of net ecosystem exchange into assimilation and ecosystem respiration: review and improved algorithm. Glob Chang Biol 11:1424–1439. doi:10.1111/j.1365-2486.2005.001002.x

Ruehr NK, Knohl A, Buchmann N (2009) Environmental variables controlling soil respiration on diurnal, seasonal and annual time-scales in a mixed mountain forest in Switzerland. Biogeochemistry 98:153–170. doi:10.1007/s10533-009-9383-z

Savage K, Davidson EA, Tang J (2013) Diel patterns of autotrophic and heterotrophic respiration among phenological stages. Glob Chang Biol 19:1151–1159. doi:10.1111/gcb.12108

Sparks D, Page A, Helmke P, et al. (1996) Methods of soil analysis - Part 3: Chemical methods. 1309

Subke J-A, Bahn M (2010) On the "temperature sensitivity" of soil respiration: can we use the immeasurable to predict the unknown? Soil Biol Biochem 42:1653–1656

Vargas R, Detto M, Baldocchi DD, Allen MF (2010) Multiscale analysis of temporal variability of soil $CO_2$ production as influenced by weather and vegetation. Glob Chang Biol 16:1589–1605. doi:10.1111/j.1365-2486.2009.02111.x

Vargas R, Baldocchi DD, Bahn M et al (2011) On the multi-temporal correlation between photosynthesis and soil $CO_2$ efflux: reconciling lags and observations. New Phytol 191:1006–17. doi:10.1111/j.1469-8137.2011.03771.x

Verma AK, Kelleners TJ (2012) Depthwise carbon dioxide production and transport in a rangeland soil. Soil Sci Soc Am J 76:821–828. doi:10.2136/sssaj2011.0416

Wang Q, Tenhunen J, Dinh NQ et al (2004) Similarities in ground- and satellite-based NDVI time series and their relationship to physiological activity of a Scots pine forest in Finland. Remote Sens Environ 93:225–237. doi:10.1016/j.rse.2004.07.006

Wang W, Peng S, Fang J (2010) Root respiration and its relation to nutrient contents in soil and root and EVI among 8 ecosystems, northern China. Plant Soil 333:391–401. doi:10.1007/s11104-010-0354-x